Supplement of Atmos. Chem. Phys., 17, 5311–5329, 2017
http://www.atmos-chem-phys.net/17/5311/2017/
doi:10.5194/acp-17-5311-2017-supplement

Atmospheric Chemistry and Physics
Open Access
EGU

Supplement of

Influence of fuel ethanol content on primary emissions and secondary aerosol formation potential for a modern flex-fuel gasoline vehicle

Hilkka Timonen et al.

Correspondence to: Hilkka Timonen (hilkka.timonen@fmi.fi)

Supplemental material includes:

Sections:

S1. Driving cycle and car preparation

S2. OH reactivity

S3. PM and vapour losses in PAM chamber

Figures:

Figure S1: Measurement setup

Figure S2. NEDC driving cycle

Figure S3: Primary particle losses in a similar PAM chamber that was used in the study

Figure S4: The composition and concentration (mg/km) of emitted primary (a) and secondary (b) PM for each fuel.

Figures S5-S16: The average mass spectra over the NEDC cycle as well as time series of all main components (organics, rBC, inorganic ions) during the NEDC cycle for all fuels (E10, E85, E100) with and without a PAM chamber

Figure S17: the ratios with PAM chamber to w/o PAM chamber ratios for C_2-C_5 fragments for E10.

Figure S18-S19: Average number and volume size distributions measured for different fuels (E10, E85, E100) with and without PAM chamber

Figures S20-S22: The predicted SOA formation potentials of CSUDC (0-391 s) for all fuels.

Figure S23: Comparison between measured and predicted SOA formation potential.

Tables:

Table S1: Regulated emissions (average ± st.dev) during the NEDC cycle

Tables S2-S4: The average OH reactivities (OHR) during different parts of the cycle for all fuels are presented in Tables include the OHR for each compound is its concentration times the reaction rate constant with OH.

Table S5: Increase in the HRLPI mass due to PAM particle wall-loss correction

Table S6: Detection limits as a ppm and mg/km for compounds measured with the FTIR.

Table S7: LVOC fate in the PAM chamber

S1. Driving cycle and car preparation

Cold-start tests were carried out by using the European exhaust emissions driving cycle, "NEDC" (Fig. S2), which is defined in the UN ECE R83 regulation. NEDC totals 11.0 km and is divided into three test phases to study emissions at cold start and with warmed-up engines. The first (Cold start urban driving cycle, CSUDC) and second test phases (hot start urban driving cycle, HUDC) each consists of 2.026 km driving, and the third test phase, the extra-urban driving cycle (EUDC), is 6.955 km. Preparation needs and stability issues related to the FFV cars were based in the earlier project (Aakko-Saksa et al., 2014). After the fuel change and prior to NEDC, a hot-start test was applied to monitor how warmed-up cars performed. For this purpose, the FTP75 city driving cycle was run as a hot-start test (FTP75 cold-start procedure is defined by the US Environmental Protection Agency EPA). FTP75 driving cycle totals 17.77 km, which is divided into three test phases including a 600 seconds pause. Before the FTP75 hot-start test, a "dummy" test FTP75 was conducted to stabilize cars for the actual hot-start test. Thereby, preparation of cars before the cold-start NEDC test on the following test day to avoid carry-over effect was extensive. Two NEDC tests were conducted for each fuel. Table S1 includes the concentrations of regulated emissions (average ± st.dev) during the driving cycle.

S2. OH reactivity

The average OH reactivities (OHR) during different parts of the cycle for all fuels are presented in Tables S2-S4. The OHR for each compound is its concentration times the reaction rate constant with OH. The rate constants are taken from Atkinson and Arey (2003) and Li et al. (2015). The different parts of the driving cycle are defined as CSUDC (0-391 s), HUDC (392-787 s) and EUDC (788-1180 s).

S3. PM and vapour losses in PAM chamber

S3.1 PM losses

PAM chamber was designed with lower surface-area-to-volume (SA/V) ratio to minimize wall effects. Primary particle losses represented in Fig. S3, were measured in laboratory for a similar PAM chamber as was used in this study. Losses were in general quite small in the particle sizes that contains most of the aerosol mass: 25% at 50 nm, 15% at 100 nm and below 10% above 150 nm.

The particle number size distributions measured by HR-LPI were used to estimate how the particle losses in the PAM affect the measured total particle mass. If the measured HR-LPI number size distributions are corrected with the particle loss curve (Fig. S3), the total mass calculated from the number size distribution increases by 9-16 % depending on the phase of the cycle and the fuel (Table S5).

S3.2 Vapour losses

The secondary aerosol is formed when low volatility vapors condense on aerosols or form new particles. In the PAM chamber, these vapors may also condense onto walls, exit the chamber, or react with OH, which leads to fragmentation and increase in the saturation vapor pressure. Thus the potential aerosol mass is underestimated if these chamber related losses of low volatile vapors are not taken into account. We used the LVOC (low volatility organic compound) fate model presented by Palm et al. (2016) to estimate the losses of condensing organic vapors in the PAM chamber (model available at https://sites.google.com/site/pamwiki/hardware/estimation-equations). In the model, the relative fates of the vapor are estimated by studying the timescales of condensation on particles, condensation on chamber walls, reaction with OH radical and the residence time in the PAM chamber. Detailed description of the model can be found in Palm et al. (2016). Shortly: The lifetime for LVOC condensation is

$$\tau_{aer} = \frac{1}{4\pi \cdot CS \cdot D},$$

where D is the diffusion coefficient of the condensing molecule and CS is the condensational sink, which is calculated using the average of the HRLPI size distributions before and after PAM. The rate of LVOC loss to the walls is

$$\frac{1}{\tau_{wall}} = \frac{A}{V}\frac{2}{\pi}\sqrt{k_e D},$$

where A/V is the surface-area-to-volume ratio of the chamber, k_e is the coefficient of eddy diffusion and D the diffusion coefficient.

The assumptions used in the model are same as in Palm et al. (2016): $D = 7 \times 10^{-6}\ m^2 s^{-1}$, $\alpha = 1$, mean free path $\lambda_g = 3\sqrt{\frac{\pi m_g}{8kT}} D \approx 1.173 \times 10^{-7}\ m$ (Pirjola et al. 1999), $\frac{A}{V} = 25\ m^{-1}$ and $k_e = 0.0036\ s^{-1}$.

The reaction rate constant for the reaction with OH is $k_{OH} = 1 \times 10^{-11}\ cm^3\ molec.^{-1}\ s^{-1}$. LVOC is considered to fragment and form high-volatility molecules after five reactions with OH radical. Thus, the lifetime for fragmentation is

$$\tau_{OH} = \frac{5}{k_{OH} \cdot [OH]},$$

where [OH] is calculated based on the OH exposure and the residence time.

Using these lifetimes, the fate of LVOCs was calculated for each fuel and each part of the driving cycle, and the results are presented in Table S7. Because of the high condensational sink, over 95 % of the LVOCs condensed on aerosol in all cases according to this model. Thus, the chamber related losses of LVOCs are small.

Figures:

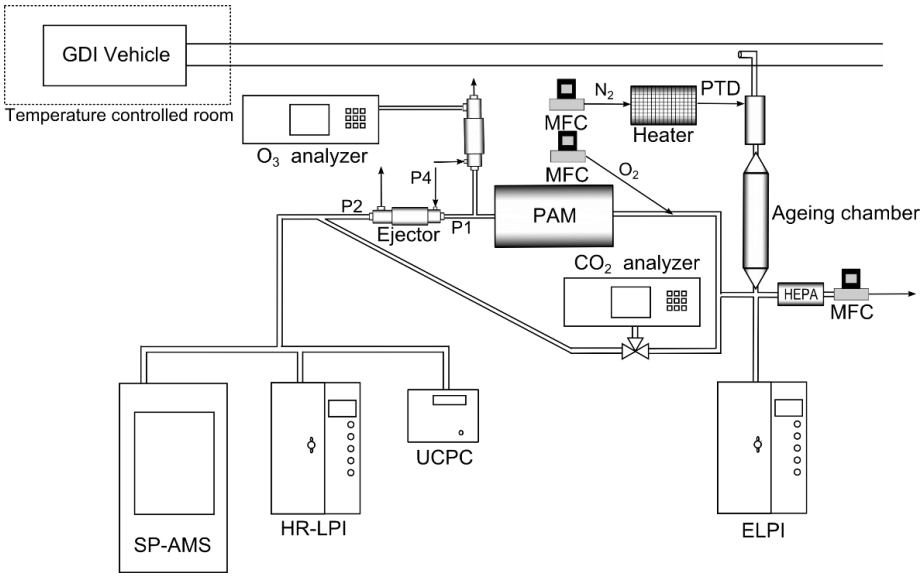

Figure S1. Experimental setup (MFC = mass flow controller) used in this campaign. (Figure adapted from Karjalainen et al., 2016 with permission).

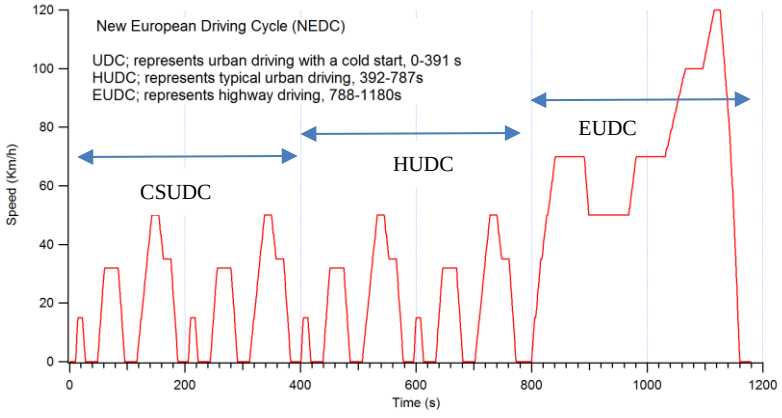

Figure S2: NEDC driving cycle

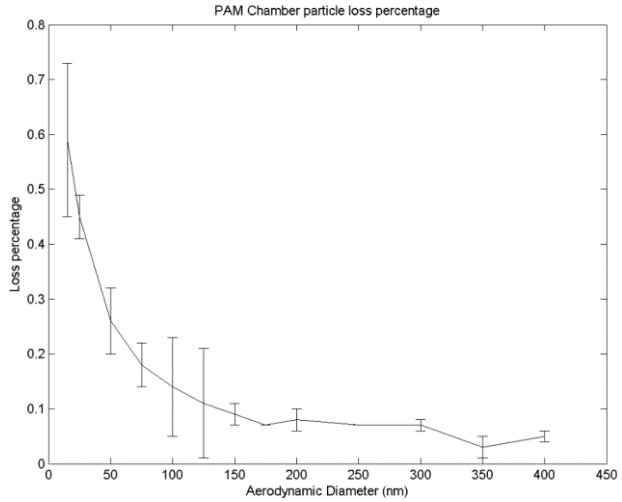

Figure S3. Primary particle loss ratio vs in a similar PAM chamber that was used in the study. (Figure adapted from Karjalainen et al., 2016 with permission).

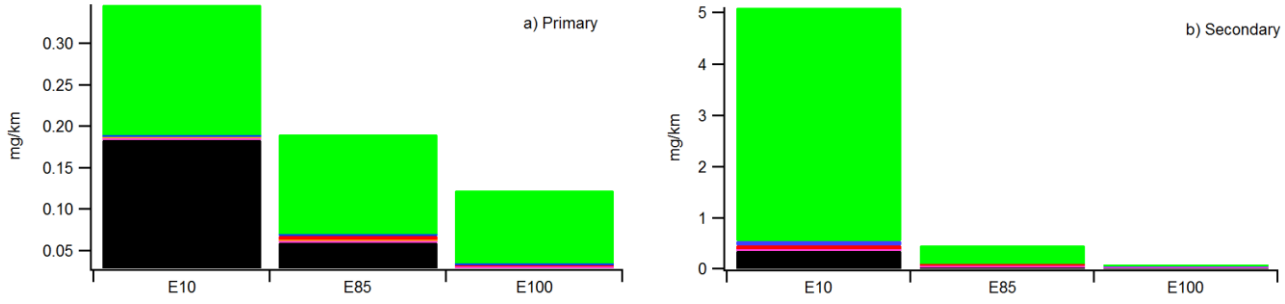

Figure S4: The composition and concentration (mg/km) of emitted primary (a) and secondary (b) PM for each fuel.

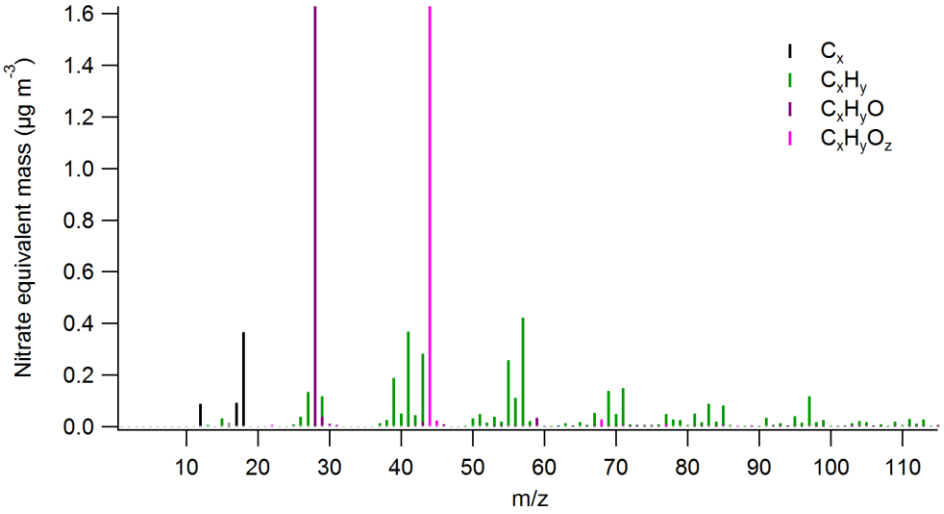

Figure S5: Average mass spectra for primary emissions of E10 during the NEDC cycle.

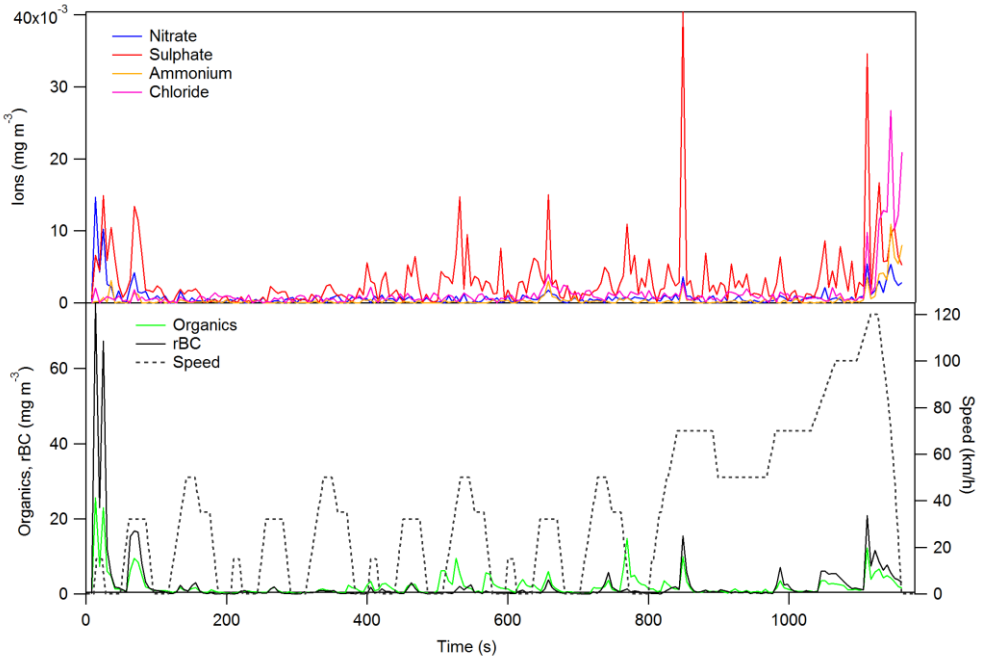

Figure S6: Timeseries of primary organic, inorganic (sulfate, ammonium, nitrate, chloride) compounds and rBC during the NEDC cycle when using E10 fuel.

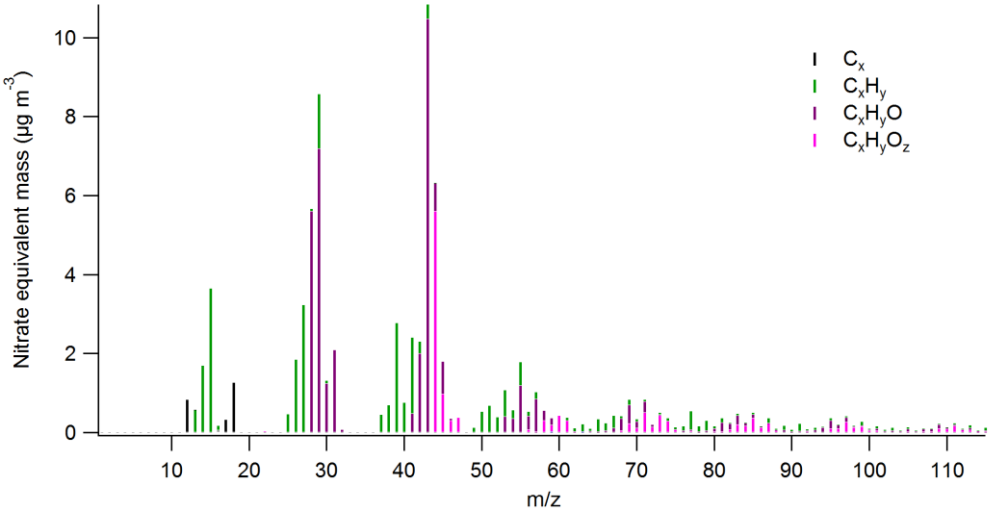

Figure S7. Average mass spectra over the NEDC cycle for E10 secondary emissions

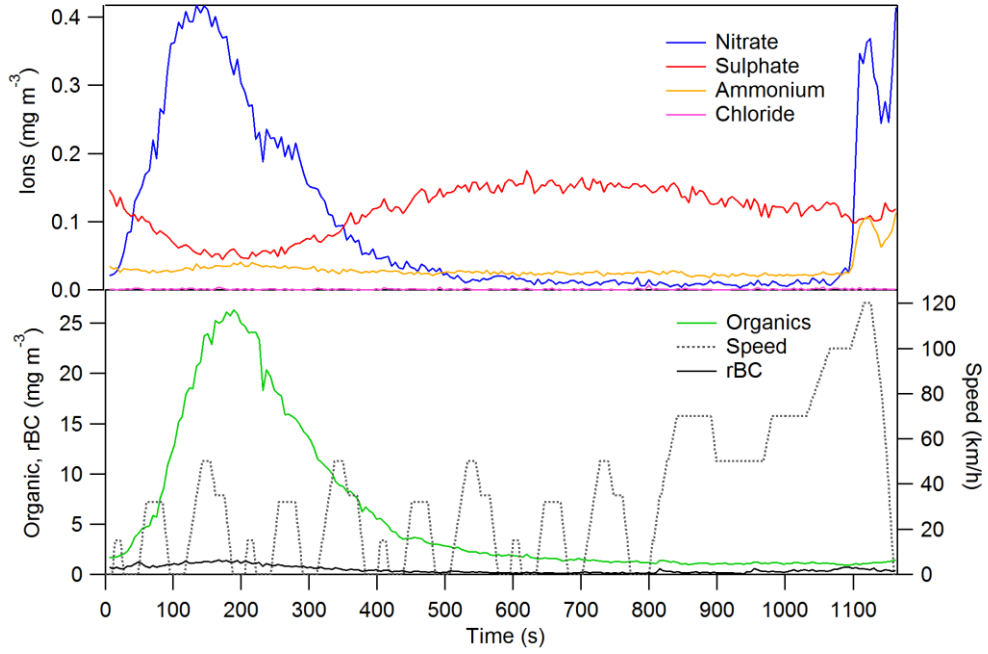

Figure S8: Timeseries of PM organic, inorganic (sulfate, ammonium, nitrate, chloride) compounds and rBC observed after PAM chamber during the NEDC cycle when using E10 fuel.

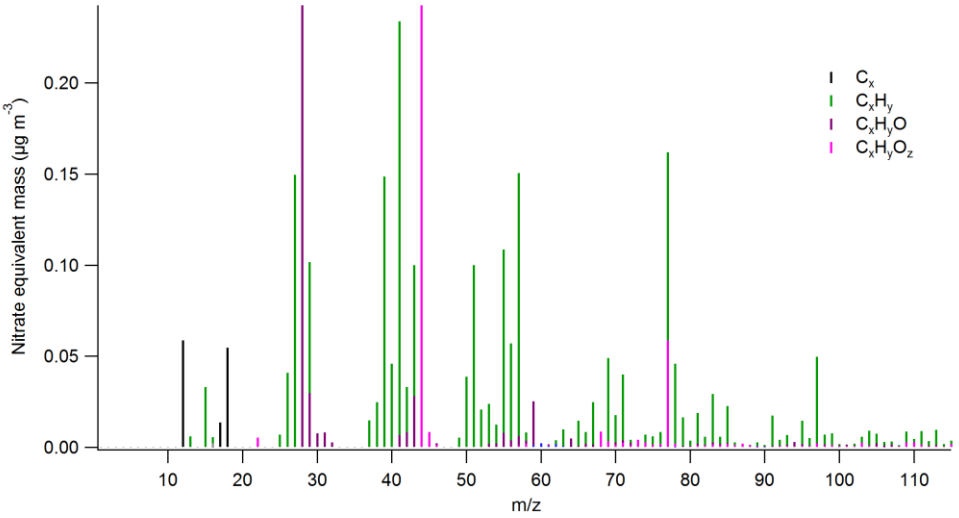

Figure S9: Average mass spectra over the NEDC cycle for E85 primary emissions

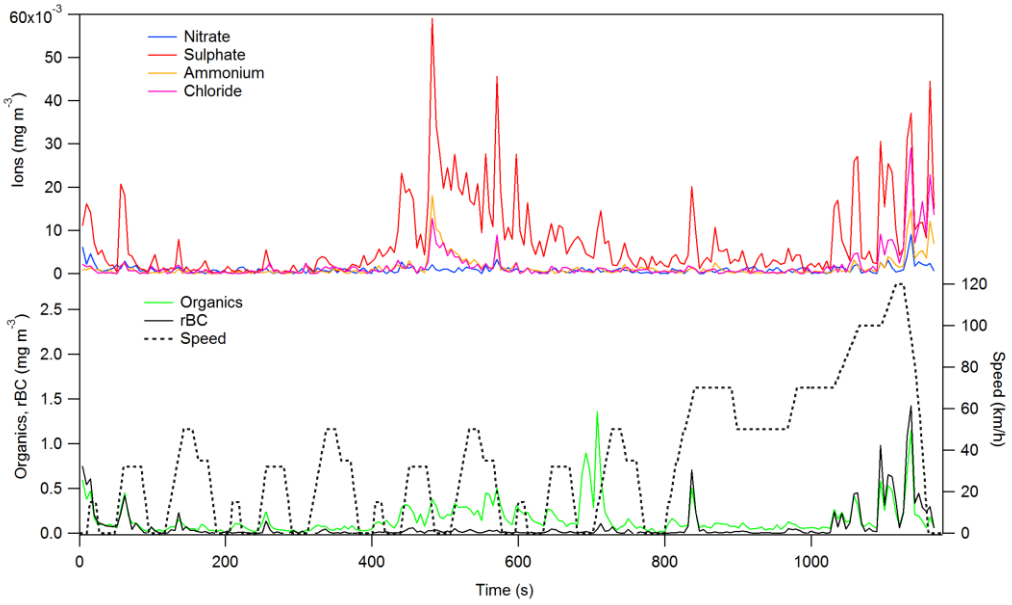

Figure S10: Timeseries of primary organic, inorganic (sulfate, ammonium, nitrate, chloride) compounds and rBC during the NEDC cycle when using E85 fuel.

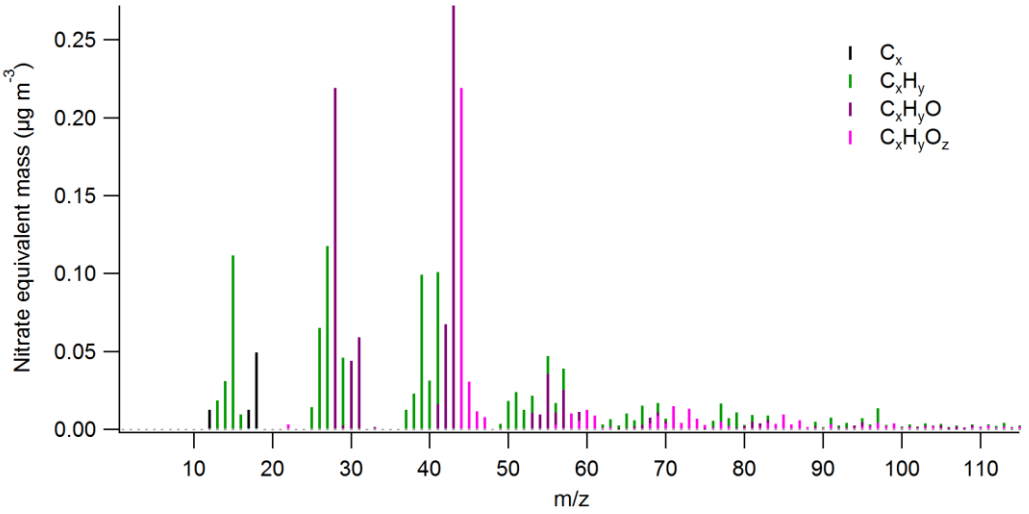

Figure S11: Average mass spectra over the NEDC cycle for E85 secondary emissions

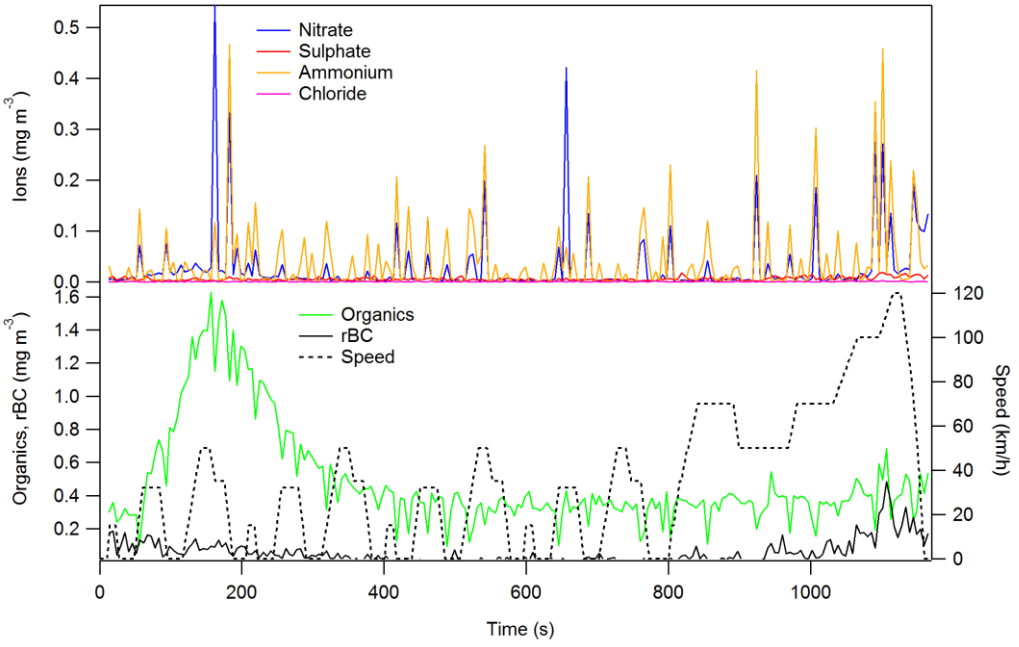

Figure S12: Timeseries of organic, inorganic (sulfate, ammonium, nitrate, chloride) compounds and rBC measured after PAM chamber during the NEDC cycle when using E85 fuel.

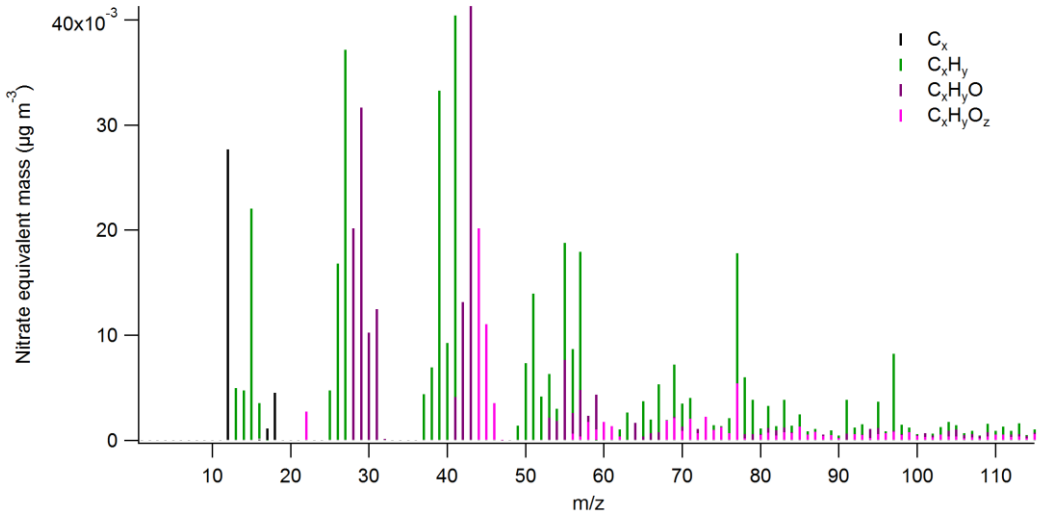

Figure S13: Average mass spectra over the NEDC cycle for E100 secondary emissions

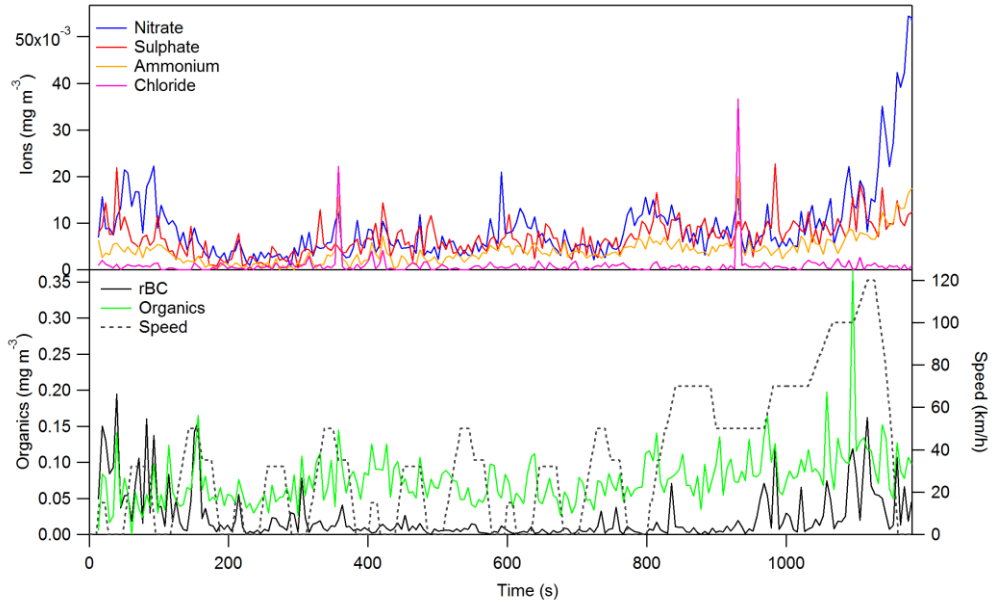

Figure S14: Timeseries of organic, inorganic (sulfate, ammonium, nitrate, chloride) compounds and rBC after PAM chamber during the NEDC cycle when using E100 fuel.

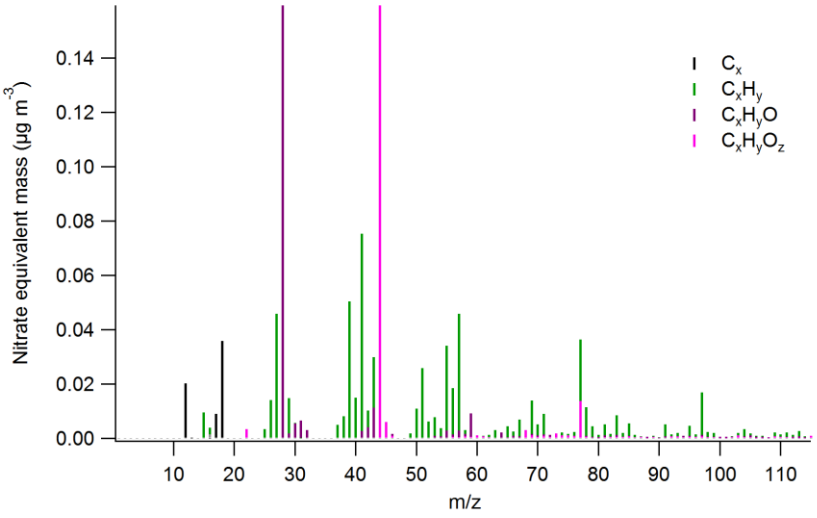

Figure S15: Average mass spectra over the NEDC cycle for E100 primary emissions

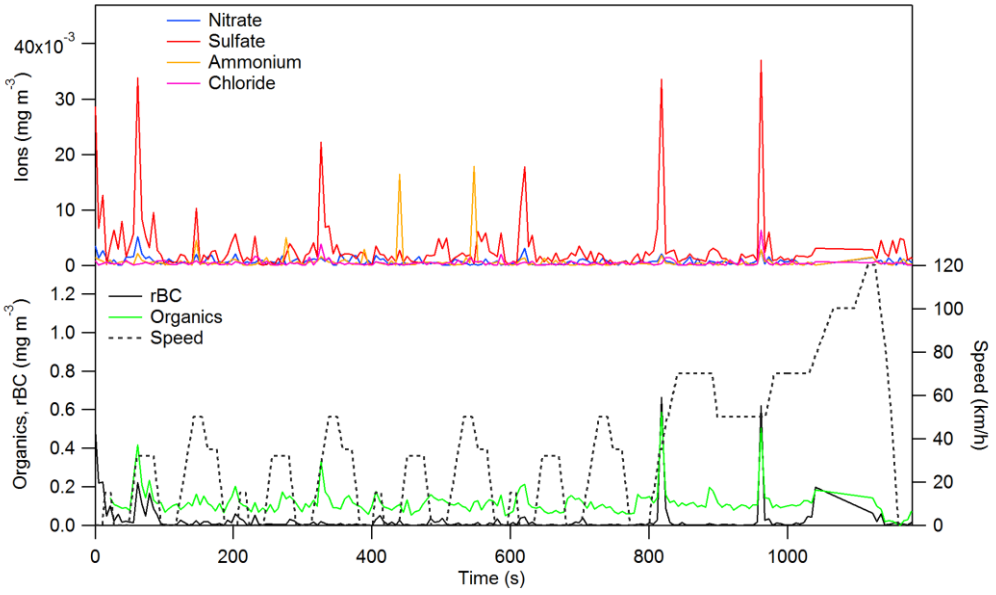

Figure S16: Timeseries of organic, inorganic (sulfate, ammonium, nitrate, chloride) compounds and rBC during the NEDC cycle when using E100 fuel.

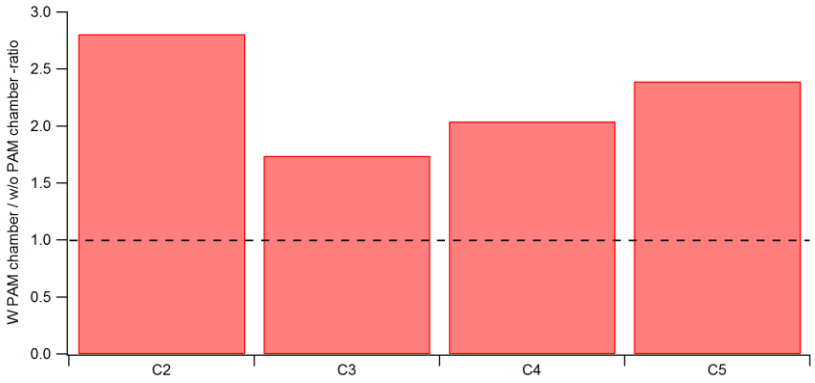

Fig S17. With PAM chamber to w/o PAM chamber ratios for C_2-C_5 fragments for E10.

5

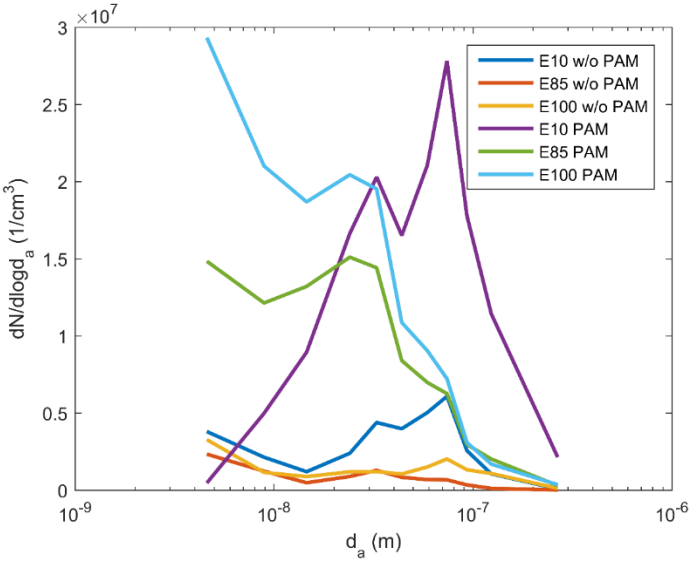

Figure S18. Average number size distributions measured for different fuels (E10, E85, E100) with and without PAM chamber.

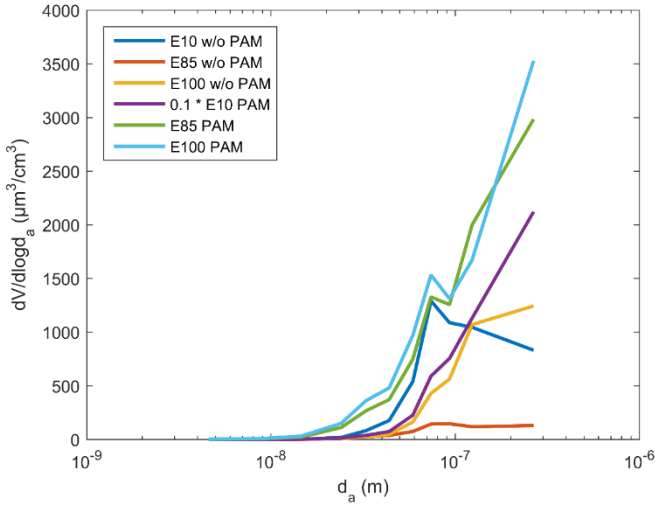

Figure S19. Average volume size distributions measured for different fuels (E10, E85, E100) with and without PAM chamber. Note the scaling by a factor 0.1 for E10 size distribution.

5

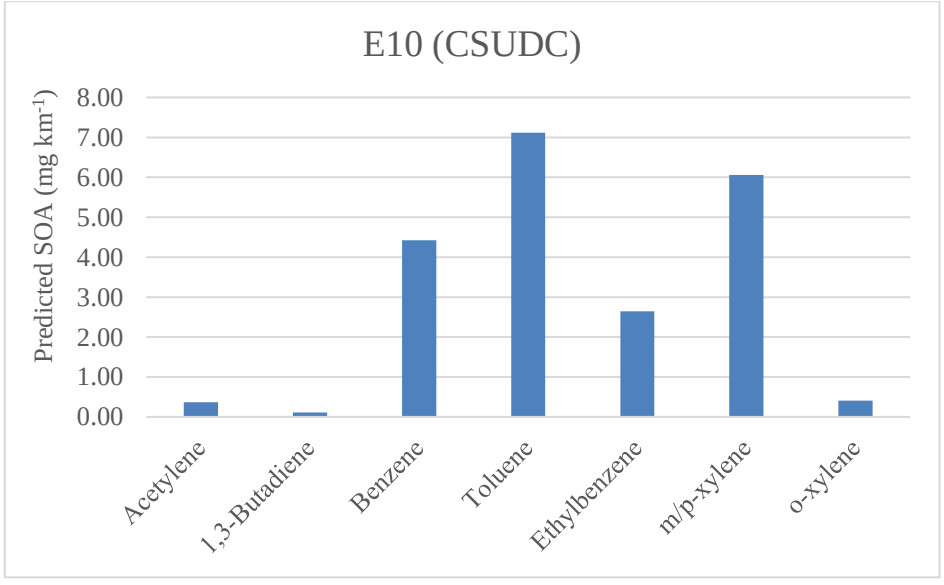

Figure S20. Predicted SOA during CSUDC for E10 fuel and low-NOx yields.

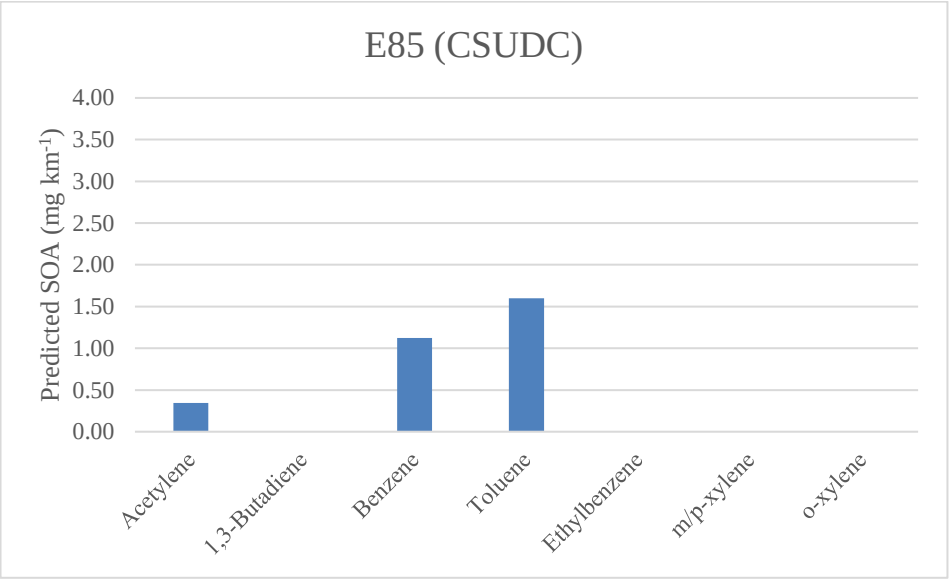

Figure S21. Predicted SOA during CSUDC for E85 fuel and low-NOx yields..

Figure S22. Predicted SOA during CSUDC for E100 fuel and low-NOx yields..

5

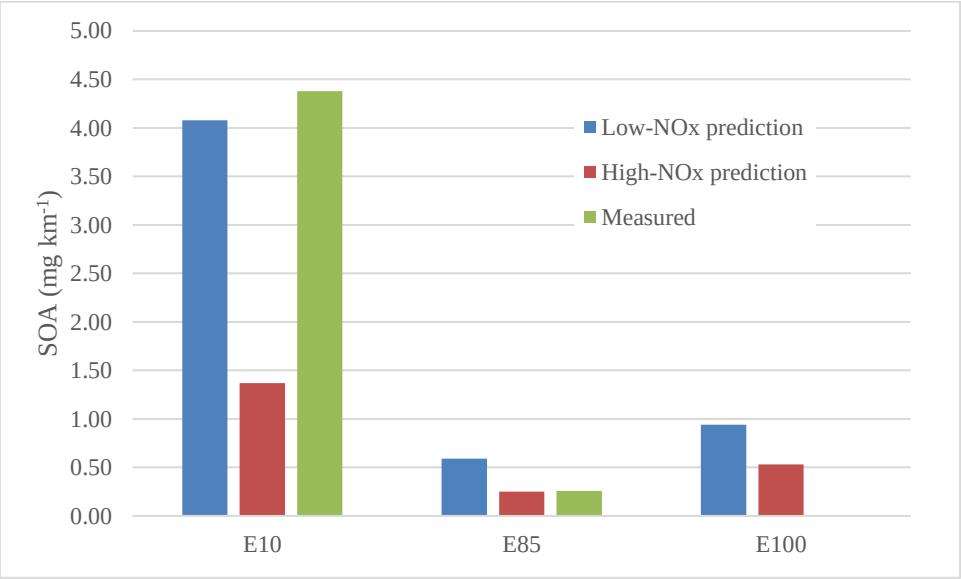

Figure S23. Comparison between measured and predicted SOA formation potential. The predictions are based on VOC measurements and SOA yields as described in Sect. 3.5.

Tables:

Table S1. Emissions (average ± st.dev) over the cold-start European test cycle (mg/km).

	Fuel	CO	HC	NOx	PM	CO2
Concentration	E10	396.6	30.4	43.3	1.4	174 181
	E85	142.1	29.9	30.3	1.3	165 837
	E100	368.2	192.9	31.7	0.9	165 196
Standard deviation						
	E10	±80.52	±10.02	±2.76	±0.08	2 729
	E85	±15.33	±2.96	±1.00	±0.64	727
---	E100	±187.57	±109.4	±16.51	±0.01	1 292

Table S2. OHR and predicted SOA for E10 fuel.

		Concentration			OHR			Predicted SOA (Low-NOx)				Predicted SOA (High-NOx)			
	Rate constant	CSUDC	HUDC	EUDC	CSUDC	HUDC	EUDC	Yield	CSUDC	HUDC	EUDC	Yield	CSUDC	HUDC	EUDC
	cm3 molec.-1 s-1	molec. cm-3	molec. cm-3	molec. cm-3	s-1	s-1	s-1		mg km-1	mg km-1	mg km-1		mg km-1	mg km-1	mg km-1
Methane	6.40E-15	4.58E+13	1.24E+13	6.73E+12	0	0	0	0.00	0.00	0.00	0.00	0.00	0.00	0.00	0.00
Ethane	2.48E-13	5.74E+12	0.00E+00	0.00E+00	1	0	0	0.00	0.00	0.00	0.00	0.00	0.00	0.00	0.00
Ethene	8.52E-12	1.91E+13	0.00E+00	0.00E+00	163	0	0	0.00	0.00	0.00	0.00	0.00	0.00	0.00	0.00
Propane	1.09E-12	0.00E+00	0.00E+00	0.00E+00	0	0	0	0.00	0.00	0.00	0.00	0.00	0.00	0.00	0.00
Propene	2.63E-11	4.63E+12	0.00E+00	0.00E+00	122	0	0	0.00	0.00	0.00	0.00	0.00	0.00	0.00	0.00
Acetylene	8.80E-13	7.52E+12	0.00E+00	0.00E+00	7	0	0	0.10	0.37	0.00	0.00	0.10	0.37	0.00	0.00
Iso-butene	5.14E-11	2.02E+12	0.00E+00	0.00E+00	104	0	0	0.00	0.00	0.00	0.00	0.00	0.00	0.00	0.00
1,3-Butadiene	6.66E-11	6.20E+11	0.00E+00	0.00E+00	41	0	0	0.18	0.11	0.00	0.00	0.18	0.11	0.00	0.00
Benzene	1.22E-12	4.50E+12	0.00E+00	1.56E+11	5	0	0	0.67	4.42	0.00	0.10	0.35	2.32	0.00	0.05
Toluene	5.63E-12	7.17E+12	1.27E+11	1.63E+11	40	1	1	0.57	7.11	0.10	0.10	0.15	1.83	0.03	0.03
Ethylbenzene	7.00E-12	1.98E+12	0.00E+00	0.00E+00	14	0	0	0.67	2.65	0.00	0.00	0.35	1.39	0.00	0.00
m/p-xylene	1.87E-11	4.42E+12	0.00E+00	0.00E+00	83	0	0	0.68	6.06	0.00	0.00	0.10	0.85	0.00	0.00
o-xylene	1.36E-11	2.02E+12	0.00E+00	0.00E+00	28	0	0	0.10	0.41	0.00	0.00	0.05	0.20	0.00	0.00
CO	2.37E-13	2.50E+15	5.69E+13	3.38E+14	593	14	80	0.00	0.00	0.00	0.00	0.00	0.00	0.00	0.00
Formaldehyde	9.37E-12	2.60E+12	6.12E+11	3.40E+11	24	6	3	0.00	0.00	0.00	0.00	0.00	0.00	0.00	0.00
Acetaldehyde	1.50E-11	1.10E+12	1.78E+11	1.16E+11	17	3	2	0.00	0.00	0.00	0.00	0.00	0.00	0.00	0.00
Ethanol	2.90E-12	1.37E+12	0.00E+00	0.00E+00	4	0	0	0.00	0.00	0.00	0.00	0.00	0.00	0.00	0.00
				SUM	1246	23	86		21.13	0.10	0.20		7.09	0.03	0.08
				Total predicted SOA						4.08 mg km-1				1.37 mg km-1	

Table S3. OHR and predicted SOA for E85 fuel.

		Concentration			OHR			Predicted SOA (Low-NOx)				Predicted SOA (High-NOx)			
	Rate constant	CSUDC	HUDC	EUDC	CSUDC	HUDC	EUDC	Yield	CSUDC	HUDC	EUDC	Yield	CSUDC	HUDC	EUDC
	cm3 molec.-1 s-1	molec. cm-3	molec. cm-3	molec. cm-3	s-1	s-1	s-1		mg km-1	mg km-1	mg km-1		mg km-1	mg km-1	mg km-1
Methane	6.40E-15	1.83E+14	1.92E+13	6.17E+12	1	0	0	0.00	0.00	0.00	0.00	0.00	0.00	0.00	0.00
Ethane	2.48E-13	0.00E+00	0.00E+00	0.00E+00	0	0	0	0.00	0.00	0.00	0.00	0.00	0.00	0.00	0.00
Ethene	8.52E-12	3.56E+13	0.00E+00	0.00E+00	304	0	0	0.00	0.00	0.00	0.00	0.00	0.00	0.00	0.00
Propane	1.09E-12	0.00E+00	0.00E+00	0.00E+00	0	0	0	0.00	0.00	0.00	0.00	0.00	0.00	0.00	0.00
Propene	2.63E-11	1.20E+12	0.00E+00	0.00E+00	31	0	0	0.00	0.00	0.00	0.00	0.00	0.00	0.00	0.00
Acetylene	8.80E-13	6.66E+12	0.00E+00	0.00E+00	6	0	0	0.10	0.34	0.00	0.00	0.10	0.34	0.00	0.00
Iso-butene	5.14E-11	0.00E+00	0.00E+00	0.00E+00	0	0	0	0.00	0.00	0.00	0.00	0.00	0.00	0.00	0.00
1,3-Butadiene	6.66E-11	0.00E+00	0.00E+00	0.00E+00	0	0	0	0.18	0.00	0.00	0.00	0.18	0.00	0.00	0.00
Benzene	1.22E-12	1.09E+12	0.00E+00	0.00E+00	1	0	0	0.67	1.12	0.00	0.00	0.35	0.59	0.00	0.00
Toluene	5.63E-12	1.54E+12	3.14E+10	3.14E+10	9	0	0	0.57	1.60	0.03	0.02	0.15	0.41	0.01	0.01
Ethylbenzene	7.00E-12	0.00E+00	0.00E+00	0.00E+00	0	0	0	0.67	0.00	0.00	0.00	0.35	0.00	0.00	0.00
m/p-xylene	1.87E-11	0.00E+00	0.00E+00	0.00E+00	0	0	0	0.68	0.00	0.00	0.00	0.10	0.00	0.00	0.00
o-xylene	1.36E-11	0.00E+00	0.00E+00	0.00E+00	0	0	0	0.10	0.00	0.00	0.00	0.05	0.00	0.00	0.00
CO	2.37E-13	9.82E+14	8.18E+12	1.16E+14	233	2	28	0.00	0.00	0.00	0.00	0.00	0.00	0.00	0.00
Formaldehyde	9.37E-12	5.46E+12	1.54E+12	5.50E+11	51	14	5	0.00	0.00	0.00	0.00	0.00	0.00	0.00	0.00
Acetaldehyde	1.50E-11	2.43E+13	2.22E+11	2.21E+11	364	3	3	0.00	0.00	0.00	0.00	0.00	0.00	0.00	0.00
Ethanol	2.90E-12	4.83E+13	4.71E+12	3.33E+12	140	14	10	0.00	0.00	0.00	0.00	0.00	0.00	0.00	0.00
				SUM	1140	34	46		3.07	0.03	0.02		1.35	0.01	0.01
				Total predicted SOA						0.59 mg km-1				0.25 mg km-1	

Table S4. OHR and predicted SOA for E100 fuel.

		Concentration			OHR			Predicted SOA (Low-NOx)				Predicted SOA (High-NOx)			
	Rate constant	CSUDC	HUDC	EUDC	CSUDC	HUDC	EUDC	Yield	CSUDC	HUDC	EUDC	Yield	CSUDC	HUDC	EUDC
	cm3 molec.-1 s-1	molec. cm-3	molec. cm-3	molec. cm-3	s-1	s-1	s-1		mg km-1	mg km-1	mg km-1		mg km-1	mg km-1	mg km-1
Methane	6.40E-15	2.93E+14	2.61E+13	9.16E+12	2	0	0	0.00	0.00	0.00	0.00	0.00	0.00	0.00	0.00
Ethane	2.48E-13	0.00E+00	0.00E+00	0.00E+00	0	0	0	0.00	0.00	0.00	0.00	0.00	0.00	0.00	0.00
Ethene	8.52E-12	1.03E+14	0.00E+00	0.00E+00	880	0	0	0.00	0.00	0.00	0.00	0.00	0.00	0.00	0.00
Propane	1.09E-12	0.00E+00	0.00E+00	0.00E+00	0	0	0	0.00	0.00	0.00	0.00	0.00	0.00	0.00	0.00
Propene	2.63E-11	1.46E+12	0.00E+00	0.00E+00	38	0	0	0.00	0.00	0.00	0.00	0.00	0.00	0.00	0.00
Acetylene	8.80E-13	2.07E+13	8.74E+11	3.55E+11	18	1	0	0.10	1.11	0.04	0.01	0.10	1.11	0.04	0.01
Iso-butene	5.14E-11	0.00E+00	0.00E+00	0.00E+00	0	0	0	0.00	0.00	0.00	0.00	0.00	0.00	0.00	0.00
1,3-Butadiene	6.66E-11	0.00E+00	0.00E+00	0.00E+00	0	0	0	0.18	0.00	0.00	0.00	0.18	0.00	0.00	0.00
Benzene	1.22E-12	6.05E+11	3.12E+11	1.01E+11	1	0	0	0.67	0.64	0.27	0.06	0.35	0.34	0.14	0.03
Toluene	5.63E-12	7.26E+11	5.20E+11	9.62E+10	4	3	1	0.57	0.78	0.45	0.06	0.15	0.20	0.12	0.02
Ethylbenzene	7.00E-12	0.00E+00	1.12E+12	0.00E+00	0	8	0	0.67	0.00	1.31	0.00	0.35	0.00	0.69	0.00
m/p-xylene	1.87E-11	0.00E+00	0.00E+00	0.00E+00	0	0	0	0.68	0.00	0.00	0.00	0.10	0.00	0.00	0.00
o-xylene	1.36E-11	0.00E+00	0.00E+00	0.00E+00	0	0	0	0.10	0.00	0.00	0.00	0.05	0.00	0.00	0.00
CO	2.37E-13	1.30E+15	4.85E+13	1.77E+14	309	12	42	0.00	0.00	0.00	0.00	0.00	0.00	0.00	0.00
Formaldehyde	9.37E-12	1.19E+13	1.15E+12	7.52E+11	111	11	7	0.00	0.00	0.00	0.00	0.00	0.00	0.00	0.00
Acetaldehyde	1.50E-11	8.24E+13	5.05E+11	4.23E+11	1237	8	6	0.00	0.00	0.00	0.00	0.00	0.00	0.00	0.00
Ethanol	2.90E-12	2.90E+14	8.42E+12	6.46E+12	841	24	19	0.00	0.00	0.00	0.00	0.00	0.00	0.00	0.00
				SUM	3441	66	75		2.53	2.06	0.14		1.65	0.98	0.06
				Total predicted SOA						0.94 mg km-1				0.53 mg km-1	

Table S5: Detection limits as a ppm and mg/km for compounds measured with the FTIR.

	Detection limit	
	Concentration at 1-s interval (ppm)	European test (mg/km)
Carbon monoxide (CO)	7	8
Nitric oxide (NO)	13	15
Nitrogen dioxide (NO_2)	2/10	4
Nitrous oxide (N_2O)	4	4
Ammonia	2	1
Methanol	2	1
Ethanol	4	7
Isobutanol	3	9
n-Butanol	4	12
ETBE	2	8
Formaldehyde	5	6
Acetaldehyde	5	9

Table S6: Increase in the HRLPI mass due to PAM particle wall-loss correction

Fuel	CSUDC	HUDC	EUDC
E10	9 %	13 %	13 %
E85	13 %	16 %	16 %
E100	15 %	16 %	16 %

Table S7: LVOC fate in the PAM chamber.

	E10			E85			E100		
	CSUDC	HUDC	EUDC	CSUDC	HUDC	EUDC	CSUDC	HUDC	EUDC
Condense on aerosol	99.3 %	98.6 %	98.6 %	97.1 %	95.5 %	95.6 %	95.2 %	95.6 %	95.7 %
Condense on walls	0.5 %	0.5 %	0.5 %	2.3 %	2.7 %	2.6 %	3.7 %	2.4 %	2.0 %
Fragmentation	0.2 %	0.9 %	0.9 %	0.6 %	1.8 %	1.8 %	0.7 %	2.0 %	2.3 %
Exit the chamber	0.0 %	0.0 %	0.0 %	0.0 %	0.0 %	0.0 %	0.3 %	0.0 %	0.0 %

References

Aakko-Saksa, P., Rantanen-Kolehmainen, L. and Skyttä, E. Ethanol, Isobutanol, and Biohydrocarbons as Gasoline Components in Relation to Gaseous Emissions and Particulate Matter. Environmental Science & Technology. American Chemical Society. Vol. 48 (2014) No: 17, 10489 – 10496. doi: 10.1021/es501381h.

Atkinson, R., and Arey, J.: Atmospheric Degradation of Volatile Organic Compounds, Chemical Reviews, 103, 4605-4638, 10.1021/cr0206420, 2003.

Karjalainen, P., Timonen, H., Saukko, E., Kuuluvainen, H., Saarikoski, S., Aakko-Saksa, P., Murtonen, T., Bloss, M., Dal Maso, M., Simonen, P., Ahlberg, E., Svenningsson, B., Brune, W. H., Hillamo, R., Keskinen, J., and Rönkkö, T.: Time-resolved characterization of primary particle emissions and secondary particle formation from a modern gasoline passenger car, Atmos. Chem. Phys., 16, 8559-8570, 10.5194/acp-16-8559-2016, 2016

Li, R., Palm, B.B., Ortega, A.M., Hlywiak, J., Hu, W., Peng, Z., Day, D.A., Knote, C., Brune, W.H., de Gouw, J.A., and Jimenez, J.L.: Modeling the Radical Chemistry in an Oxidation Flow Reactor: Radical Formation and Recycling, Sensitivities, and the OH Exposure Estimation Equation, The Journal of Physical Chemistry, 119, 4418-4432, 10.1021/jp509534k, 2015.

Ortega, A. M., Hayes, P. L., Peng, Z., Palm, B. B., Hu, W., Day, D. A., Li, R., Cubison, M. J., Brune, W. H., Graus, M., Warneke, C., Gilman, J. B., Kuster, W. C., de Gouw, J., Gutiérrez-Montes, C. and Jimenez, J. L.: Real-time measurements of secondary organic aerosol formation and aging from ambient air in an oxidation flow reactor in the Los Angeles area, Atmos. Chem. Phys., 16(11), 7411–7433, doi:10.5194/acp-16-7411-2016, 2016.

Palm, B. B., Campuzano-Jost, P., Ortega, A. M., Day, D. A., Kaser, L., Jud, W., Karl, T., Hansel, A., Hunter, J. F., Cross, E. S., Kroll, J. H., Peng, Z., Brune, W. H. and Jimenez, J. L.: In situ secondary organic aerosol formation from ambient pine forest air using an oxidation flow reactor, Atmos. Chem. Phys., 16(5), 2943–2970, doi:10.5194/acp-16-2943-2016, 2016.